


## Article

# Reduced Mechanism for Combustion of Ammonia and Natural Gas Mixtures

Aniket R. Khade <sup>1</sup>, Vijaya D. Damodara <sup>2</sup> and Daniel H. Chen <sup>3,\*</sup> 
<sup>1</sup> Flutura, 5858 Westheimer Suite 405, Houston, TX 77057, USA

<sup>2</sup> John Zink Hamworthy Combustion, 11920 E Apache St., Tulsa, OK 74116, USA

<sup>3</sup> Dan F. Smith Department of Chemical Engineering, Lamar University, Beaumont, TX 77710, USA

\* Correspondence: daniel.chen@lamar.edu

**Abstract:** A fuel mixture of ammonia and natural gas as a low-carbon alternative for future power generation and transportation is an attractive option. In this work, a 50-species reduced mechanism, NH<sub>3</sub>NG, suitable for computational fluid dynamics simulations (CFD), is developed for ammonia–natural gas cofiring while addressing important emission issues, such as the formation of nitrogen oxides (NO<sub>x</sub>), soot, carbon monoxide, and unburnt methane/ammonia. The adoption of reduced mechanisms is imperative not only for saving computer storage and running time but also for numerical convergence for practical applications. The NH<sub>3</sub>NG reduced mechanism can predict soot emission because it includes soot precursor species. Further, it can handle heavier components in natural gas, such as ethane and propane. The absolute error is 5% for predicting NO<sub>x</sub> and CO emissions compared to the full Modified Konnov mechanism. Validation with key performance parameters (ignition delay, laminar flame speed, adiabatic temperature, and NO<sub>x</sub> and CO emissions) indicates that the predictions of the reduced mechanism NH<sub>3</sub>NG are in good agreement with published experimental data. The average prediction error of 13% for ignition delay is within typical experimental data uncertainties of 10–20%. The predicted adiabatic temperatures are within 1 °C. For laminar flame speed, the R<sup>2</sup> between prediction and data is 0.985. NH<sub>3</sub>NG over-predicts NO<sub>x</sub> and CO emissions, similar to all other literature methods, but the NO<sub>x</sub> predictions are closer to the experimental data.

**Keywords:** reduced mechanism; ammonia; natural gas; combustion; soot; nitrogen oxides



**Citation:** Khade, A.R.; Damodara, V.D.; Chen, D.H. Reduced Mechanism for Combustion of Ammonia and Natural Gas Mixtures. *Clean Technol.* **2023**, *5*, 484–496. <https://doi.org/10.3390/cleantechnol5020025>

Academic Editors: Hong Duc Pham, Deepak Dubal and Nilesh Chodankar

Received: 11 October 2022

Revised: 10 March 2023

Accepted: 10 April 2023

Published: 12 April 2023



**Copyright:** © 2023 by the authors. Licensee MDPI, Basel, Switzerland. This article is an open access article distributed under the terms and conditions of the Creative Commons Attribution (CC BY) license (<https://creativecommons.org/licenses/by/4.0/>).

## 1. Introduction

Since wind and solar power sources are intermittent in nature and are generally far from urban centers, there is a compelling need to store large quantities of renewable energy with a faster response. The popular power from hydrogen concept via a water splitter can be used to create ammonia by reacting hydrogen with nitrogen in an air separation unit (ASU). Ammonia is currently manufactured at a large scale as an industrial chemical and fertilizer. Owing to its various merits—ammonia (1) is easy to store as a liquid; similar to propane; (2) has a high energy density; and (3) handling experience and infrastructure are already available—nowadays, ammonia is widely considered as an important hydrogen-carrier for future marine shipping or commercial aviation to drive turbines or engines, Figure 1. Ammonia can be easily cracked back to pure hydrogen for those applications that use pure hydrogen or a mix of hydrogen with other fuels, including ammonia itself [1–6].

However, through fuel NO<sub>x</sub> mechanisms, nitrogen-containing ammonia can lead to significant NO<sub>x</sub> emissions. Further, there are also concerns about unburnt ammonia and slow ammonia kinetics at low temperatures. On the other hand, using natural gas (NG) as a fuel has distinct advantages, such as

- (1) Higher hydrogen content relative to gasoline, diesel, and coal;
- (2) High adiabatic flame temperature and high laminar flame speed;
- (3) Well-established infrastructure;
- (4) Abundance of natural gas reserves in the US.
- (5) A worldwide increase in liquefied natural gas (LNG) plants and terminals.

Because of the above-mentioned advantages, cofiring ammonia with natural gas has gained significant attention as a clean source of energy in gas turbines for power generation as well as in internal combustion engines (ICE) for transportation. Even though cofiring ammonia with natural gas can ease the above-mentioned emission concerns of combusting ammonia alone, additional emissions, such as soot, carbon monoxide, unburnt hydrocarbons, and Volatile Organic Compounds (VOCs), still need to be addressed [7–19].

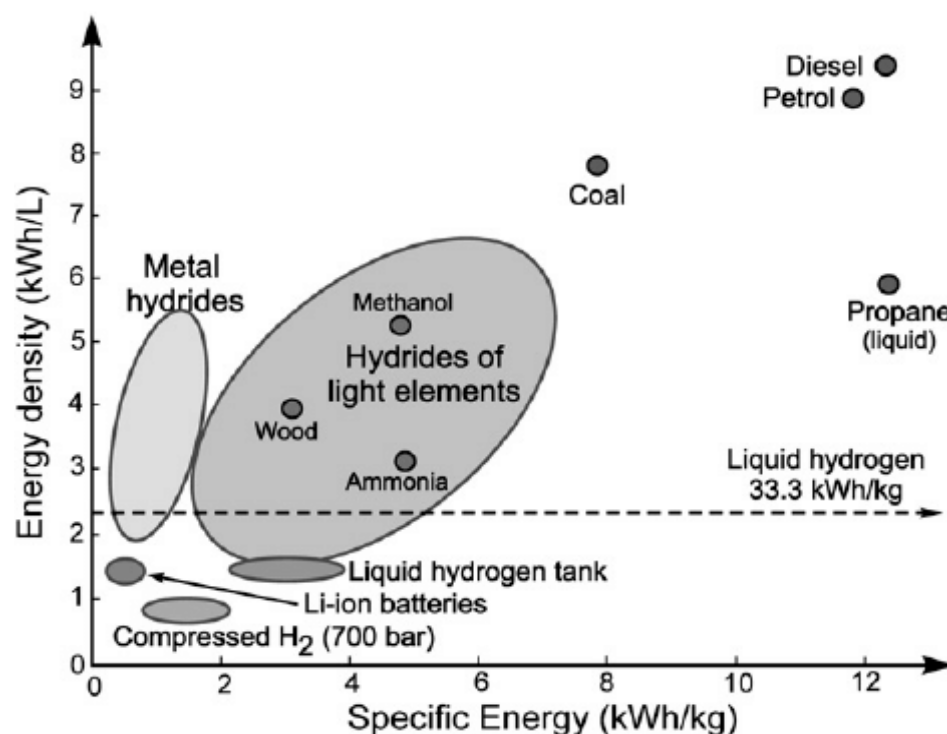


**Figure 1.** Ammonia energy density chart [3].

There are full mechanisms in the literature that address combustion involving ammonia in the air. The detailed Konnov mechanism for ammonia consists of 129 species and 957 reactions [11]. A new version of the Konnov model targeting the ammonia flame and an improved hydrocarbon subset has also been reported [13,14]. The CEU-NH<sub>3</sub> mechanism for ammonia and methane/methanol/ethanol contains 91 species and 444 reactions [15]. The UC San Diego mechanisms are a suite of mechanisms, including nitrogen and hydrocarbon-based chemistry [16]. The USCII full mechanism, developed by Professor Hai Wang, is a detailed kinetic mechanism tailored for hydrogen and C<sub>1</sub> to C<sub>4</sub> combustion with 111 species in 784 reversible reactions [17–19].

The objective of this study is to develop a reaction mechanism that can be used in computational fluid dynamics' (CFD) modeling to predict NO<sub>x</sub>/soot/unburnt NH<sub>3</sub>/unburnt hydrocarbons/volatile organic compound (VOC) emissions under gas turbine and internal combustion engine (ICE) conditions. The Konnov and the USCII mechanisms [10,17–19] were combined to become the full mechanism (Modified Konnov Mechanism). The full Konnov mechanism has 129 species. Additional species (C<sub>4</sub>H<sub>10</sub>, pC<sub>4</sub>H<sub>9</sub>, and nC<sub>3</sub>H<sub>7</sub>) and associated mechanisms from USCII were added to the Konnov mechanism to make the Modified Konnov Mechanism, which has 132 species and 1238 reactions.

Reduced mechanisms are required for practical turbine/ICE applications due to the complexity of 3D computational fluid dynamics' (CFD) simulations. The CFD simulations are widely used in turbine, engine, and furnace design for analyzing flame stability, autoignition zone, temperature/velocity profiles, fuel/oxidizer mixing patterns, and emission rates. However, coupling detailed reaction mechanisms with momentum, heat, mass transport equations, and stiff differential equations proved to be a serious burden on computational speed and numerical convergence. Thus, it is imperative to adopt reduced mechanisms not only for saving computer storage and running time but also for numerical convergence for practical applications. For instance, ANSYS Fluent sets the maximum number of species in the reactions to 50. One of the goals of this paper is to contribute an ammonia–methane cofiring reduced mechanism that can handle heavier hydrocarbons ( $C_2$  and  $C_3$ ) in natural gas streams, Table 1. Further, many existing reduced mechanisms for ammonia and methane mixtures are unsuitable for predicting soot emissions. Therefore, the developed reduced mechanism  $NH_3NG$  also included soot precursor species  $C_2H_2$  and  $C_2H_4$  to facilitate soot emission estimation.  $NH_3NG$  compares well with the full mechanism and existing reduced mechanisms when validated against experimental ignition delay, adiabatic temperature, laminar flame speed, and  $NO_x/CO$  emissions [20–33].

**Table 1.** Natural gas composition [4].

Component	Typical (%)	Range (Mole)
Methane	94.9	87.0–96.0
Ethane	2.5	1.8–5.1
$C^{3+}$	0.3	0.1–2.3
Nitrogen	1.6	1.3–5.6
Carbon	0.7	0.1–1.0

## 2. Methodology

The mechanism reduction was performed using Chemkin 2019 R2 [33–36]. The following steps were taken to determine the 50 species to be included in the reduced mechanism  $NH_3NG$ :

1. The species in the reduced mechanism should be suitable for the targeted applications in turbine/engine design with CFD. In this study, the reduced mechanism should include fuel species, emission species ( $NO$ ,  $NO_2$ ,  $NH_3$ ,  $HCN$ ,  $N_2O$ ), and soot precursors ( $C_2H_2$ ,  $C_2H_4$ ).
2. The next step is to utilize the Reaction Path Analyzer (RPA) tool in Chemkin. RPA provides a visualization of the inner relationships of the chemistry model, as shown in Figure 2.
3. The final step in species selection is to apply the Reaction Rate Analysis (RRA) tool. In this Chemkin analysis, the Perfectly Stirred Reactor (PSR) model is adopted. In these PSR runs, the species with a higher rate of production or destruction are expected to be dominant in the reaction mechanism and, thus, are ranked higher. Both RPA and RRA are needed to identify important intermediate species for  $NH_3NG$  to represent the essential elements of the full Modified Konnov Mechanism.

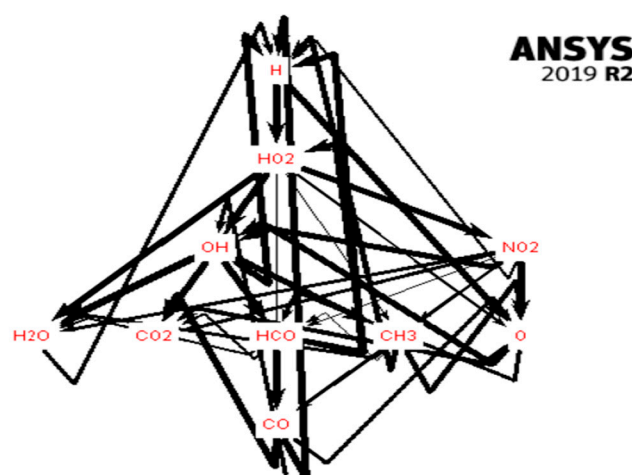


**Figure 2.** Reaction path analyzer (RPA) for the production of CO with the line thickness proportional to the rate of reactions.

### 2.1. Preliminary Species Selection

Mechanism reduction was conducted at a temperature of 1500 K and pressure of 300 bar, using Chemkin 2019 R2 [36]. For the reduced mechanism, the initial species list included Fuel Species ( $\text{NH}_3$ ,  $\text{CH}_4$ ,  $\text{C}_2\text{H}_6$ ,  $\text{C}_3\text{H}_8$ ),  $\text{NO}_x$  and  $\text{NO}_y$  ( $\text{NO}$ ,  $\text{NO}_2$ ,  $\text{HONO}$ ), Soot Precursors ( $\text{C}_2\text{H}_2$ ,  $\text{C}_2\text{H}_4$ ), and Air ( $\text{O}_2$ ,  $\text{N}_2$ ,  $\text{Ar}$ ).

The soot precursor species  $\text{C}_2\text{H}_2$  and  $\text{C}_2\text{H}_4$  are important in that the soot emission can be predicted with precursor-based soot models, such as the Moss–Brookes' equation (with the built-in Fenimore–Jones soot oxidation model) listed in ANSYS Fluent [26–32]. Additional species ( $\text{C}$ ,  $\text{CH}$ ,  $\text{CH}_2$ ,  $\text{C}_3\text{H}_3$ , and  $\text{C}_4\text{H}_4$ ) were also included as they were part of the reaction intermediates.

### 2.2. Reaction Path Analyzer (RPA)

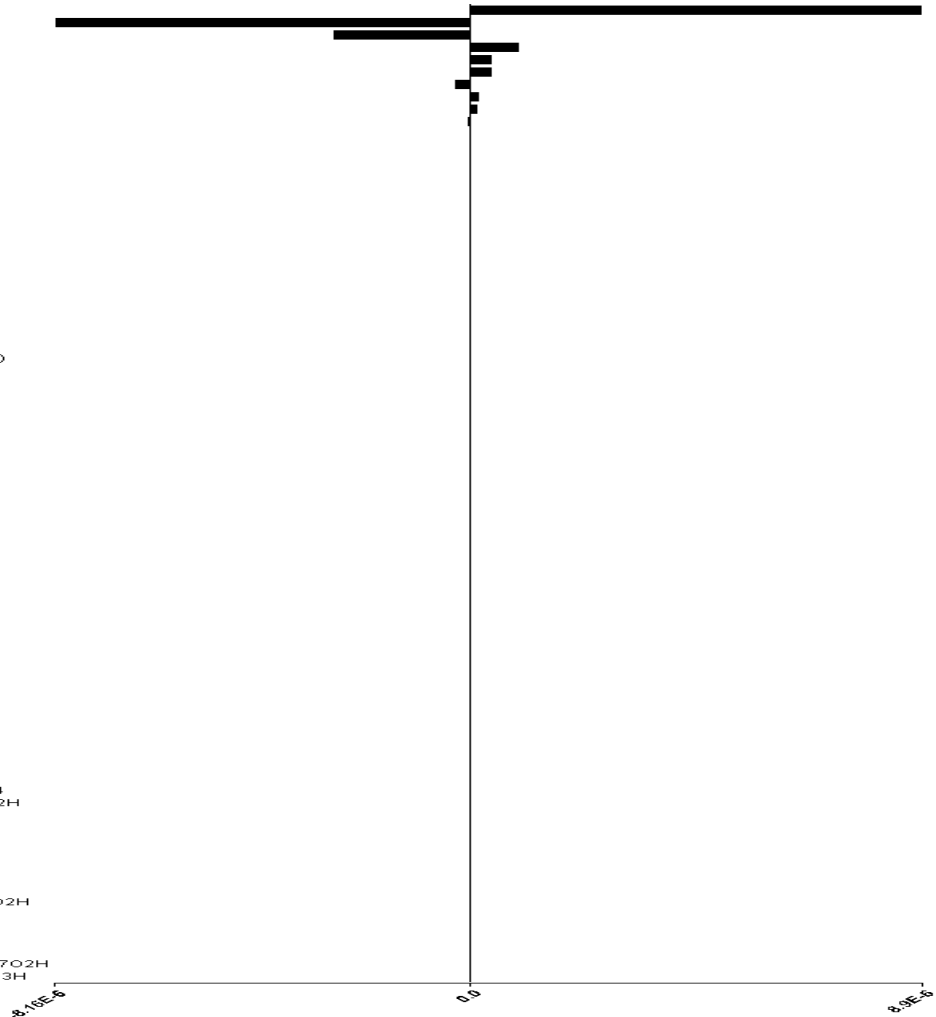
The reaction path analyzer (RPA) displays reaction pathways connecting the species. Since the path width is proportional to its rate of production, RPA helps identify the main intermediates during reactions and eliminates any species with negligible contributions [28]. In this study, reaction paths between fuel components and the major intermediates/products ( $\text{CO}$ ,  $\text{CO}_2$ ,  $\text{NO}$ ,  $\text{NO}_2$ ,  $\text{C}_2\text{H}_4$ ) were analyzed. The major contributing reactions and participating species were identified. Figure 2 shows the reaction pathways for CO production.

### 2.3. Reaction Rate Analysis (RRA)

The important intermediate species were selected based on the active participation of the species in the reaction. To determine the key intermediate species, the production and destruction rates were added and sorted to obtain the ranks of the species. The species with a higher rate of production or destruction were ranked higher. From the rankings list, it was observed that most of the species were already included in the reduced mechanism. However, some species, such as  $\text{C}$ ,  $\text{CH}$ ,  $\text{CH}_2$ ,  $\text{C}_3\text{H}_3$ , and  $\text{C}_4\text{H}_4$ , were still needed (e.g., for soot production). Therefore, they were subsequently added to the list, and the mechanism was reduced further. Figure 3 gives the reaction rate analysis for the key intermediate  $\text{C}_2\text{H}_4$ , a soot precursor species. Table 2 shows the final 50 selected species.

Absolute Rate of Production C<sub>2</sub>H<sub>4</sub>

C<sub>2</sub>H<sub>5</sub>(+M) <=> C<sub>2</sub>H<sub>4</sub>+H(+M)  
 C<sub>2</sub>H<sub>4</sub>+OH <=> C<sub>2</sub>H<sub>3</sub>+H<sub>2</sub>O  
 C<sub>2</sub>H<sub>4</sub>+OH <=> CH<sub>2</sub>O+CH<sub>3</sub>  
 NC<sub>3</sub>H<sub>7</sub> <=> C<sub>2</sub>H<sub>4</sub>+CH<sub>3</sub>  
 C<sub>2</sub>H<sub>4</sub>+OH(+M) <=> PC<sub>2</sub>H<sub>5</sub>O(+M)  
 C<sub>2</sub>H<sub>5</sub>+O<sub>2</sub> <=> C<sub>2</sub>H<sub>4</sub>+HO<sub>2</sub>  
 C<sub>2</sub>H<sub>4</sub>+M <=> C<sub>2</sub>H<sub>2</sub>+H<sub>2</sub>+M  
 C<sub>2</sub>H<sub>5</sub>O<sub>2</sub> <=> C<sub>2</sub>H<sub>4</sub>+HO<sub>2</sub>  
 C<sub>2</sub>H<sub>5</sub>+OH <=> C<sub>2</sub>H<sub>4</sub>+H<sub>2</sub>O  
 C<sub>2</sub>H<sub>4</sub>+O <=> CH<sub>3</sub>+HCO  
 C<sub>2</sub>H<sub>4</sub>+O <=> C<sub>2</sub>H<sub>3</sub>+OH  
 IC<sub>3</sub>H<sub>7</sub> <=> C<sub>2</sub>H<sub>4</sub>+CH<sub>3</sub>  
 C<sub>2</sub>H<sub>4</sub>+O <=> CH<sub>2</sub>HCO+H  
 C<sub>3</sub>H<sub>4</sub>+OH <=> HCO+C<sub>2</sub>H<sub>4</sub>  
 C<sub>3</sub>H<sub>5</sub>+O <=> C<sub>2</sub>H<sub>4</sub>+CO+H  
 C<sub>2</sub>H<sub>4</sub>+O <=> CH<sub>2</sub>CO+H<sub>2</sub>  
 C<sub>2</sub>H<sub>5</sub>OH <=> C<sub>2</sub>H<sub>4</sub>+H<sub>2</sub>O  
 C<sub>2</sub>H<sub>5</sub>+O <=> C<sub>2</sub>H<sub>4</sub>+OH  
 C<sub>2</sub>H<sub>4</sub>+M <=> C<sub>2</sub>H<sub>3</sub>+H+M  
 C<sub>2</sub>H<sub>4</sub>+HO<sub>2</sub> <=> C<sub>2</sub>H<sub>4</sub>O+OH  
 C<sub>2</sub>H<sub>5</sub>+HO<sub>2</sub> <=> C<sub>2</sub>H<sub>4</sub>+H<sub>2</sub>O<sub>2</sub>  
 C<sub>2</sub>H<sub>4</sub>+O<sub>2</sub> <=> C<sub>2</sub>H<sub>3</sub>+HO<sub>2</sub>  
 C<sub>3</sub>H<sub>6</sub>+O <=> C<sub>2</sub>H<sub>4</sub>+CH<sub>2</sub>O  
 C<sub>3</sub>H<sub>4</sub>+O <=> CO+C<sub>2</sub>H<sub>4</sub>  
 C<sub>2</sub>H<sub>4</sub>+O <=> CH<sub>2</sub>O+CH<sub>2</sub>  
 C<sub>2</sub>H<sub>4</sub>+H <=> C<sub>2</sub>H<sub>3</sub>+H<sub>2</sub>  
 C<sub>2</sub>H<sub>4</sub>+CH<sub>3</sub> <=> C<sub>2</sub>H<sub>3</sub>+CH<sub>4</sub>  
 CH<sub>2</sub>+CH<sub>3</sub> <=> C<sub>2</sub>H<sub>4</sub>+H  
 C<sub>2</sub>H<sub>5</sub>(+C<sub>2</sub>H<sub>6</sub>) <=> C<sub>2</sub>H<sub>4</sub>+H(+C<sub>2</sub>H<sub>6</sub>)  
 IC<sub>4</sub>H<sub>7</sub> <=> C<sub>2</sub>H<sub>4</sub>+C<sub>2</sub>H<sub>3</sub>  
 C<sub>2</sub>H<sub>4</sub>+HO<sub>2</sub> <=> C<sub>2</sub>H<sub>3</sub>+H<sub>2</sub>O<sub>2</sub>  
 C<sub>2</sub>H<sub>5</sub>+CH<sub>3</sub> <=> C<sub>2</sub>H<sub>4</sub>+CH<sub>4</sub>  
 SCH<sub>2</sub>+C<sub>2</sub>H<sub>4</sub> <=> C<sub>3</sub>H<sub>6</sub>  
 2CH<sub>3</sub> <=> C<sub>2</sub>H<sub>4</sub>+H<sub>2</sub>  
 C<sub>2</sub>H<sub>3</sub>+CH<sub>2</sub>O <=> C<sub>2</sub>H<sub>4</sub>+HCO  
 C<sub>2</sub>H<sub>3</sub>+C<sub>2</sub>H<sub>4</sub> <=> C<sub>4</sub>H<sub>6</sub>+H  
 CH<sub>2</sub>+C<sub>2</sub>H<sub>4</sub> <=> C<sub>3</sub>H<sub>6</sub>  
 HCCO+CH<sub>3</sub> <=> C<sub>2</sub>H<sub>4</sub>+CO  
 SCH<sub>2</sub>+CH<sub>3</sub> <=> C<sub>2</sub>H<sub>4</sub>+H  
 C<sub>2</sub>H<sub>4</sub>O+H <=> C<sub>2</sub>H<sub>4</sub>+OH  
 C<sub>2</sub>H<sub>5</sub>+H <=> C<sub>2</sub>H<sub>4</sub>+H<sub>2</sub>  
 SCH<sub>2</sub>+CH<sub>2</sub>CO <=> C<sub>2</sub>H<sub>4</sub>+CO  
 PC<sub>3</sub>H<sub>4</sub>+HO<sub>2</sub> <=> C<sub>2</sub>H<sub>4</sub>+CO+OH  
 2C<sub>2</sub>H<sub>4</sub> <=> C<sub>2</sub>H<sub>5</sub>+C<sub>2</sub>H<sub>3</sub>  
 C<sub>2</sub>H<sub>4</sub>+CH<sub>3</sub>O<sub>2</sub> <=> C<sub>2</sub>H<sub>4</sub>O+CH<sub>3</sub>O  
 C<sub>2</sub>H<sub>6</sub>+C<sub>2</sub>H<sub>3</sub> <=> C<sub>2</sub>H<sub>4</sub>+C<sub>2</sub>H<sub>5</sub>  
 C<sub>3</sub>H<sub>5</sub>+C<sub>2</sub>H<sub>5</sub> <=> C<sub>3</sub>H<sub>6</sub>+C<sub>2</sub>H<sub>4</sub>  
 C<sub>2</sub>H<sub>3</sub>+HCO <=> C<sub>2</sub>H<sub>4</sub>+CO  
 C<sub>2</sub>H<sub>4</sub>+CH<sub>3</sub>O<sub>2</sub> <=> C<sub>2</sub>H<sub>3</sub>+CH<sub>3</sub>O<sub>2</sub>H  
 C<sub>3</sub>H<sub>8</sub>+C<sub>2</sub>H<sub>3</sub> <=> NC<sub>3</sub>H<sub>7</sub>+C<sub>2</sub>H<sub>4</sub>  
 CH<sub>2</sub>CO+CH<sub>2</sub> <=> C<sub>2</sub>H<sub>4</sub>+CO  
 C<sub>4</sub>H<sub>8</sub>+O <=> CH<sub>3</sub>HCO+C<sub>2</sub>H<sub>4</sub>  
 2C<sub>2</sub>H<sub>5</sub> <=> C<sub>2</sub>H<sub>4</sub>+C<sub>2</sub>H<sub>6</sub>  
 CH+CH<sub>4</sub> <=> C<sub>2</sub>H<sub>4</sub>+H  
 C<sub>3</sub>H<sub>8</sub>+C<sub>2</sub>H<sub>3</sub> <=> IC<sub>3</sub>H<sub>7</sub>+C<sub>2</sub>H<sub>4</sub>  
 CH<sub>3</sub>O+C<sub>2</sub>H<sub>3</sub> <=> CH<sub>2</sub>O+C<sub>2</sub>H<sub>4</sub>  
 CH<sub>3</sub>O+C<sub>2</sub>H<sub>4</sub> <=> CH<sub>2</sub>O+C<sub>2</sub>H<sub>5</sub>  
 C<sub>3</sub>H<sub>5</sub>+C<sub>2</sub>H<sub>3</sub> <=> C<sub>3</sub>H<sub>4</sub>+C<sub>2</sub>H<sub>4</sub>  
 2C<sub>2</sub>H<sub>3</sub> <=> C<sub>2</sub>H<sub>2</sub>+C<sub>2</sub>H<sub>4</sub>  
 C<sub>2</sub>H<sub>4</sub>+CH<sub>3</sub>O <=> C<sub>2</sub>H<sub>3</sub>+CH<sub>3</sub>OH  
 C<sub>4</sub>H<sub>6</sub>+O <=> C<sub>2</sub>H<sub>4</sub>+CH<sub>2</sub>CO  
 C<sub>3</sub>H<sub>6</sub>+C<sub>2</sub>H<sub>3</sub> <=> C<sub>3</sub>H<sub>5</sub>+C<sub>2</sub>H<sub>4</sub>  
 C<sub>2</sub>H<sub>4</sub>+CH<sub>3</sub>O <=> C<sub>2</sub>H<sub>4</sub>O+CH<sub>3</sub>  
 CH<sub>3</sub>HCO+C<sub>2</sub>H<sub>3</sub> <=> CH<sub>3</sub>CO+C<sub>2</sub>H<sub>4</sub>  
 C<sub>2</sub>H<sub>4</sub>+C<sub>2</sub>H<sub>5</sub>O<sub>2</sub> <=> C<sub>2</sub>H<sub>3</sub>+C<sub>2</sub>H<sub>5</sub>O<sub>2</sub>H  
 TC<sub>4</sub>H<sub>8</sub>+O <=> CH<sub>3</sub>HCO+C<sub>2</sub>H<sub>4</sub>  
 C<sub>3</sub>H<sub>6</sub>+C<sub>2</sub>H<sub>3</sub> <=> SC<sub>3</sub>H<sub>5</sub>+C<sub>2</sub>H<sub>4</sub>  
 PC<sub>3</sub>H<sub>4</sub>+C<sub>2</sub>H<sub>3</sub> <=> C<sub>3</sub>H<sub>3</sub>+C<sub>2</sub>H<sub>4</sub>  
 C<sub>2</sub>C<sub>4</sub>H<sub>8</sub>+O <=> CH<sub>3</sub>HCO+C<sub>2</sub>H<sub>4</sub>  
 C<sub>3</sub>H<sub>6</sub>+C<sub>2</sub>H<sub>3</sub> <=> TC<sub>3</sub>H<sub>5</sub>+C<sub>2</sub>H<sub>4</sub>  
 TC<sub>3</sub>H<sub>5</sub>+C<sub>2</sub>H<sub>3</sub> <=> C<sub>3</sub>H<sub>4</sub>+C<sub>2</sub>H<sub>4</sub>  
 SC<sub>3</sub>H<sub>5</sub>+C<sub>2</sub>H<sub>3</sub> <=> C<sub>3</sub>H<sub>4</sub>+C<sub>2</sub>H<sub>4</sub>  
 C<sub>2</sub>H<sub>4</sub>+IC<sub>3</sub>H<sub>7</sub>O<sub>2</sub> <=> C<sub>2</sub>H<sub>3</sub>+IC<sub>3</sub>H<sub>7</sub>O<sub>2</sub>H  
 IC<sub>4</sub>H<sub>7</sub>+C<sub>2</sub>H<sub>3</sub> <=> C<sub>4</sub>H<sub>8</sub>+C<sub>2</sub>H<sub>4</sub>  
 IC<sub>4</sub>H<sub>7</sub>+C<sub>2</sub>H<sub>5</sub> <=> TC<sub>4</sub>H<sub>8</sub>+C<sub>2</sub>H<sub>4</sub>  
 IC<sub>4</sub>H<sub>7</sub>+C<sub>2</sub>H<sub>5</sub> <=> C<sub>2</sub>C<sub>4</sub>H<sub>8</sub>+C<sub>2</sub>H<sub>4</sub>  
 IC<sub>4</sub>H<sub>7</sub>+C<sub>2</sub>H<sub>5</sub> <=> C<sub>4</sub>H<sub>8</sub>+C<sub>2</sub>H<sub>4</sub>  
 C<sub>2</sub>H<sub>4</sub>+NC<sub>3</sub>H<sub>7</sub>O<sub>2</sub> <=> C<sub>2</sub>H<sub>3</sub>+NC<sub>3</sub>H<sub>7</sub>O<sub>2</sub>H  
 C<sub>2</sub>H<sub>4</sub>+CH<sub>3</sub>CO<sub>3</sub> <=> C<sub>2</sub>H<sub>3</sub>+CH<sub>3</sub>CO<sub>3</sub>H

Figure 3. Reaction rate analysis of C<sub>2</sub>H<sub>4</sub>.Table 2. Fifty (50) species of the NH<sub>3</sub>NG combustion mechanism.

50 Species	Ar N <sub>2</sub> H H <sub>2</sub> O O <sub>2</sub> OH HO <sub>2</sub> H <sub>2</sub> O CO CO <sub>2</sub> HCO CH <sub>3</sub> CH <sub>4</sub> C <sub>2</sub> H <sub>6</sub>
	CH <sub>2</sub> O C <sub>2</sub> H <sub>5</sub> CH <sub>2</sub> CH <sub>3</sub> O CH <sub>2</sub> OH CH C <sub>2</sub> H <sub>2</sub> C <sub>2</sub> H <sub>4</sub> C <sub>2</sub> H <sub>3</sub> CH <sub>3</sub> OH
	CH <sub>2</sub> CO HCCO C CH <sub>2</sub> HCO NH NO NCO N <sub>2</sub> O NH <sub>2</sub> HNO NO <sub>2</sub>
	NNH NH <sub>3</sub> HONO CNN H <sub>2</sub> NO C <sub>3</sub> H <sub>6</sub> C <sub>3</sub> H <sub>8</sub> iC <sub>3</sub> H <sub>7</sub> nC <sub>3</sub> H <sub>7</sub> C <sub>3</sub> H <sub>3</sub>
	C <sub>3</sub> H <sub>5</sub> C <sub>3</sub> H <sub>4</sub> C <sub>4</sub> H <sub>4</sub> iC <sub>4</sub> H <sub>3</sub>

### 3. Results

#### 3.1. Comparison with the Full Mechanism

The new reduced mechanism was compared against the full modified Konnov mechanism at a residence time of 1 s and ignition temperature of 1500 K, and pressure of 300 bar. The predicted mole fractions of the important combustion products obtained from the Chemkin simulation of the reduced mechanism at various residence times were recorded. Table 3 summarizes the prediction errors at a 1 s residence time for an ammonia–methane mixture. The predicted mole fraction differed from the full Modified Konnov Mechanism mole fractions by an average absolute error of  $1.90 \times 10^{-6}$  for the major species.

**Table 3.** Comparison of prediction errors of reduced mechanisms for the mole fraction of the major species at a residence time of 1 s for CH<sub>4</sub>-NH<sub>3</sub> fuel.

Species	Konnov (Modified)	NH <sub>3</sub> NG	Absolute Error	Absolute % Error
CH <sub>4</sub>	$4.85 \times 10^{-7}$	$5.34 \times 10^{-7}$	$1.10122 \times 10^{-9}$	9.99
NH <sub>3</sub>	$1.59 \times 10^{-6}$	$1.78 \times 10^{-6}$	$1.8799 \times 10^{-7}$	11.79
CO	$5.14 \times 10^{-6}$	$5.51 \times 10^{-6}$	$3.6462 \times 10^{-7}$	7.09
CO <sub>2</sub>	$6.06 \times 10^{-2}$	$6.06 \times 10^{-2}$	$3 \times 10^{-7}$	0
H <sub>2</sub>	$1.37 \times 10^{-7}$	$1.46 \times 10^{-7}$	$9.101 \times 10^{-9}$	6.65
NO <sub>2</sub>	$1.34 \times 10^{-5}$	$1.37 \times 10^{-5}$	$2.315 \times 10^{-7}$	1.72
HNO	$2.84 \times 10^{-9}$	$2.82 \times 10^{-9}$	$1.612 \times 10^{-11}$	0.57
NO	$2.48 \times 10^{-4}$	$2.34 \times 10^{-4}$	$1.41 \times 10^{-5}$	5.69
Average			$1.90 \times 10^{-6}$	5.44

The average absolute % error of 5.44% between the NH<sub>3</sub>NG reduced mechanism and modified Konnov full mechanism is reasonable, considering the goals of NH<sub>3</sub>NG are to accommodate soot prediction and to handle C<sub>2</sub>-C<sub>3</sub> hydrocarbon species. All in all, NH<sub>3</sub>NG offers a simple mechanism (with 50 species) suitable for CFD applications. The larger absolute % error of 11.79% for NH<sub>3</sub> represents the compromise between the original Konnov mechanism designed for NH<sub>3</sub> combustion and the USC II mechanism designed for hydrocarbon combustion.

### 3.2. Validation with Experimental Data

The 50 species reduced mechanism for ammonia–natural gas cofiring NH<sub>3</sub>NG was validated against key experimental performance indicators such as laminar flame speed, ignition delay, adiabatic temperature, and NO<sub>x</sub> and CO emissions [16,20,21]. The reduced mechanism containing 50 species and reactions, along with the thermodynamics file, was preprocessed using the Chemkin-Pro preprocessor. The validated reduced mechanism, NH<sub>3</sub>NG, can then be used in other ANSYS FLUENT CFD simulations [20–46].

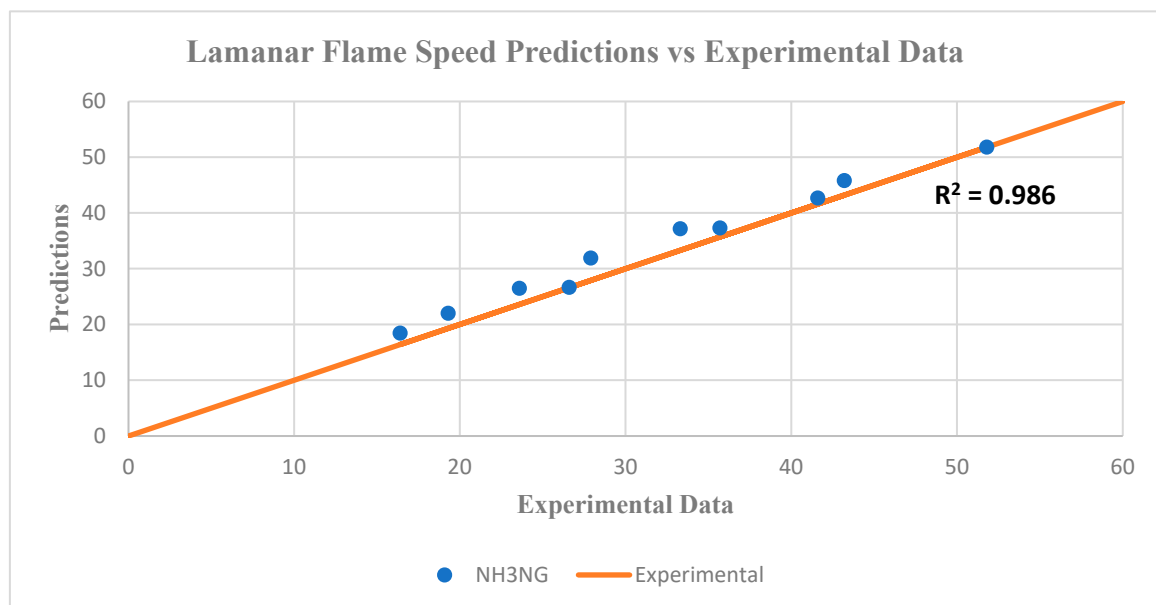
#### 3.2.1. Laminar Flame Speed

Flame speed is a fundamental property of the fuel–air mixture that influences the design of combustion equipment. Laminar flame speed is the speed at which a laminar flame propagates through a pre-mixture of fuel and air. The flame speed depends on the properties of the fuel mixture and the thermodynamic conditions, such as temperature and pressure, when ignited.

The flame speed calculation model in Chemkin was used to evaluate the performance of the reduced mechanism against the experimental values of the NH<sub>3</sub>/CH<sub>4</sub>/air system found in Rocha et al. [20]. The experimental results were used to validate the mechanism for different mixtures of ammonia and methane in the air. During validation, the temperature and pressure inside the reactor were set at 423 K and 1–3 atm., respectively. The equivalence ratio varied between 0.8 and 1.2 for all fuel mixtures. The ammonia blending fractions in the binary fuel mixtures were also varied, as shown in Table 4. The equivalence ratio is defined as the ratio of the actual fuel/oxidizer ratio to the fuel/oxidizer ratio in the stoichiometric equation. Many properties of combustion processes strongly depend on the stoichiometry of the combustion mixture. Table 4 shows an average absolute error of 7.7%, which is well within the reported experimental uncertainty of 10% [28]. As shown in Figure 4, the predicted results from the NH<sub>3</sub>NG mechanism agreed with the experimental data very well, with an R<sup>2</sup> = 0.985.

**Table 4.** Laminar flame speed predictions versus experimental data of  $\text{NH}_3/\text{CH}_4/\text{air}$  system [28].

Sr. No.	Pressure (Bar)	$x\text{NH}_3$	Equivalence Ratio	Experimental (cm/s)	$\text{NH}_3\text{NG}$ (cm/s)	Error (%)
1	3	0.2	0.8	26.6	26.6	0.1%
2	1	0.2	1	51.8	51.8	0.0%
3	2	0.2	1	41.6	42.6	2.5%
4	3	0.2	1	35.7	37.3	4.5%
5	1	0.2	1.2	43.2	45.8	6.0%
6	2	0.2	1.2	33.3	37.1	11.5%
7	3	0.2	1.2	27.9	31.9	14.3%
8	3	0.4	1.2	23.6	26.5	12.2%
9	3	0.6	1.2	19.3	22.0	14.0%
10	3	0.8	1.2	16.4	18.4	12.4%
Avg.						7.7%

**Figure 4.** Laminar flame speed predictions from  $\text{NH}_3\text{NG}$  reduced mechanism vs. experimental data.

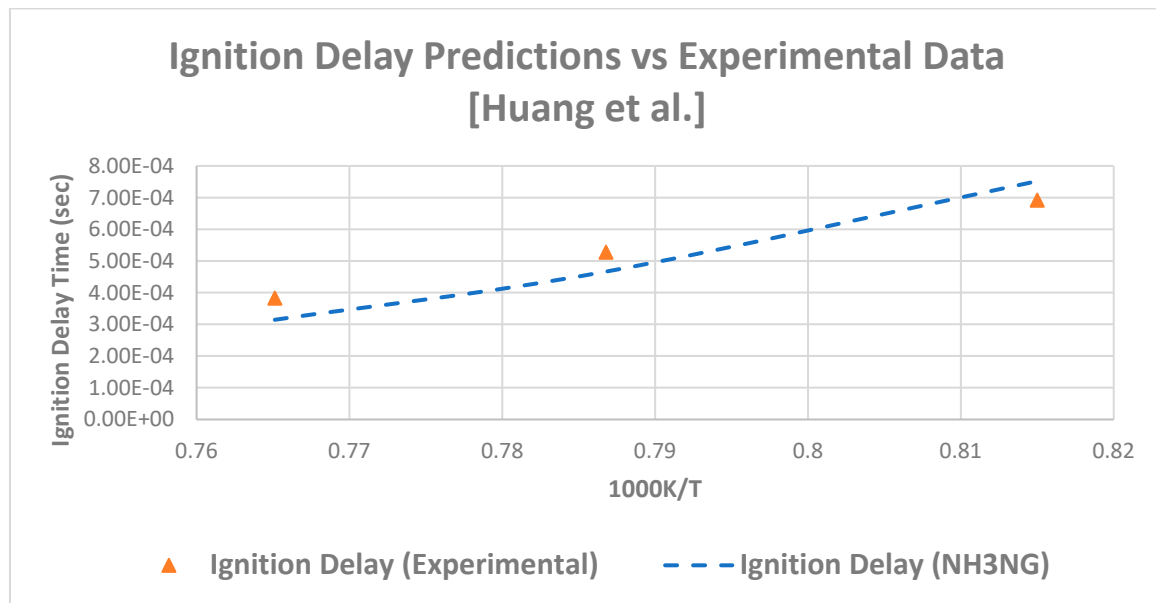
### 3.2.2. Ignition Delay

The period between the creation of a combustible mixture when the fuel is injected into an oxidizing environment and the sustained onset of the rapid reaction phase leading to a rise in temperature and pressure is defined as the ignition delay time. For ignition delay time calculations, a closed homogeneous reactor model was used. The reduced mechanism was compared against the experimental data from J. Huang et Al. [30]. For validation in Chemkin, the pressure was taken as 16 atm. and the temperature varied between 1227 and 1307 K. The fuel composition was  $\text{CH}_4/\text{C}_2\text{H}_6/\text{O}_2/\text{N}_2$  (8.93–0.34–19.05–71.68%). Table 5 shows the numerical comparison between the predictions and lab data with an average absolute error of 13%, which is well within the combined temperature/concentration uncertainties (8%) [30] and typical experimental data uncertainties (10–20%) [33]. Figure 5 shows the graphical representation of the experimental and simulation results between ignition delay time and for the said mixture with the new mechanism at the conditions mentioned above.



**Table 5.** Ignition delay time predictions versus experimental data of NH<sub>3</sub>/CH<sub>4</sub>/air system [21].

8.93% CH <sub>4</sub> , 0.34% C <sub>2</sub> H <sub>6</sub> Mixture						
Pressure (atm)	Temp (K)	1000/T	Ignition Time NH <sub>3</sub> NG (s)	Ignition Time Experimental (s)	Absolute Error	Absolute Error %
16.3	1307	0.76511	$3.15 \times 10^{-4}$	$3.83 \times 10^{-4}$	$6.85 \times 10^{-5}$	18%
15.8	1271	0.78678	$4.67 \times 10^{-4}$	$5.28 \times 10^{-4}$	$6.15 \times 10^{-5}$	12%
16.2	1227	0.815	$7.52 \times 10^{-4}$	$6.92 \times 10^{-4}$	$6.03 \times 10^{-5}$	9%
Average						13%

**Figure 5.** Ignition delay time predictions vs. experimental data [30].

### 3.2.3. Adiabatic Temperature

The adiabatic flame temperature is the maximum temperature when a particular gas mixture reaches equilibrium under an adiabatic combustion condition. In a real system, due to heat losses and chemical kinetic/mass transport limitations, the flame temperature is likely to be lower. In this validation, the adiabatic temperature was estimated with the Chemkin equilibrium model. The inlet composition of fuel and air mixtures was set at 0.8 equivalence ratios. The initial temperature and pressure were set at 293 K and 1 atm., respectively, for both fuel and air. An adiabatic flame temperature comparison of the Chemkin simulation and experimental data for ammonia and methane flames at different mole fractions of NH<sub>3</sub> is shown in Figure 6 and Table 6 [9]. As seen in Table 6, the predictions were right on target, which indicates the quality of the thermodynamic properties used in the NH<sub>3</sub>NG mechanism.

**Table 6.** Comparison of adiabatic temperature predictions and data [9].

Fuel Mixture	NH <sub>3</sub> Mole Fraction	Initial Temperature (K)	Adiabatic Temperature Exp. Data (°C) [7]	Adiabatic Temperature Prediction (°C)
NH <sub>3</sub> /CH <sub>4</sub>	0.3	293	1698	1698.4
	0.5	293	1679	1678.8
	0.7	293	1651	1651.6
	0.8	293	1634	1633.7



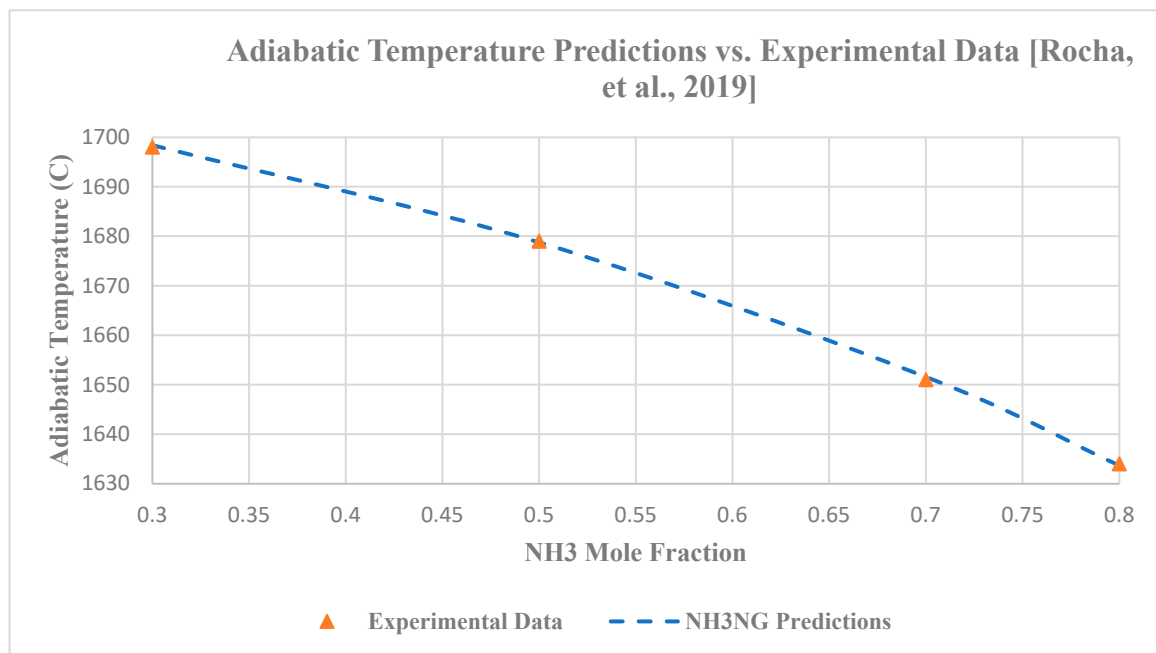


**Figure 6.** Adiabatic temperature (experimental vs. NH<sub>3</sub>NG reduced mechanism) [9].

### 3.2.4. NO<sub>x</sub> and CO Emissions

In this section, we compared the predicted NO<sub>x</sub> and CO emissions from NH<sub>3</sub>NG reduced mechanism with the experimental emission data, as well as those from different mechanisms in the literature [9,16,20,21]. These reactions were carried out in an adiabatic reactor with different CH<sub>4</sub>/NH<sub>3</sub> ratios, as shown in Table 6. The NO<sub>x</sub> and CO measurements and predictions for a thermal input of 1200 W and an equivalence ratio of 0.8 are shown in Figures 7 and 8.

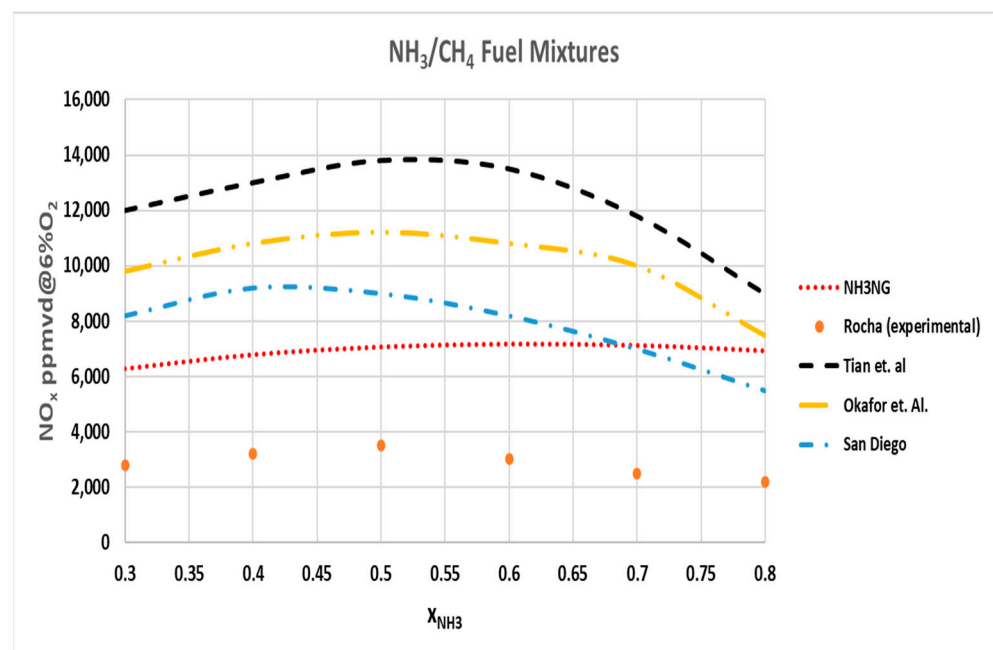


**Figure 7.** Comparison of NO<sub>x</sub> emission predictions versus NO<sub>x</sub> measurements for a thermal input of 1200 W and equivalence ratio of 0.8 [9,16,20,21].

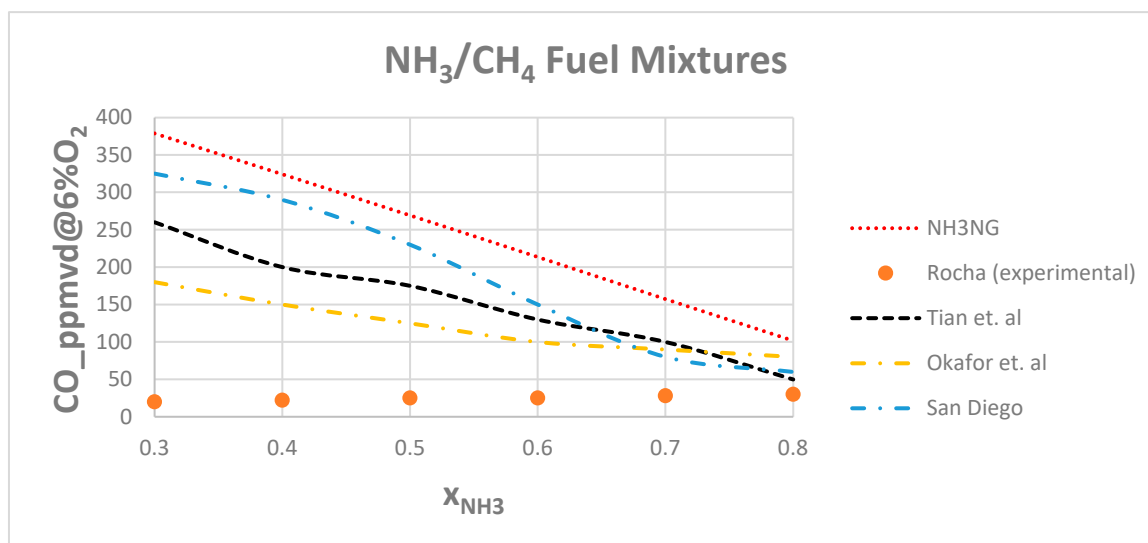


**Figure 8.** Comparison of CO emission predictions versus CO data for a thermal input of 1200 W and equivalence ratio of 0.8 [9,16,20,21].

As shown in Figures 7 and 8, all mechanisms, including the present work, over-predict NO<sub>x</sub> and CO emissions in relation to the published data available [9,16,20,21]. Overall, the predictions from the NH<sub>3</sub>NG mechanism were in line with other literature mechanisms. Compared to other mechanisms in the literature, the predicted CO emissions from NH<sub>3</sub>NG were higher (further from the experimental data). In comparison, the predicted NO<sub>x</sub> emissions were lower (closer to the experimental data).

#### 4. Discussion

Even though the mechanism reduction with Chemkin was conducted at a temperature of 1500 K and pressure of 300 bar for the purpose of developing a reduced mechanism that is useful for high-efficiency turbine and engine applications, the reduced mechanism NH<sub>3</sub>NG did remarkably well in validation at a wide range of experimental conditions, including those conducted at lower temperatures and pressures (e.g., laminar flame speed data at 423 K and 1–3 atm. [28] and ignition delay data at 16 atm. and 1227–1307 K [36]).

The Moss–Brookes model for soot prediction is applicable to higher hydrocarbon species (ethane and propane) by including appropriate soot precursors and participating surface growth species. In our earlier work of the LU 3.0.1 reduced mechanism for combustion of C<sub>1</sub> to C<sub>4</sub> light hydrocarbons, three precursor and surface growth species C<sub>2</sub>H<sub>2</sub>, C<sub>2</sub>H<sub>4</sub>, and C<sub>6</sub>H<sub>6</sub>, were involved. In this work, due to the limitation of the number of species and the addition of ammonia fuel, only two soot precursor species, C<sub>2</sub>H<sub>2</sub> and C<sub>2</sub>H<sub>4</sub>, were included in NH<sub>3</sub>NG. However, these two precursor/surface growth species were deemed sufficient to predict soot emission because even if neither is present, curve fitting can be used in Fluent to determine the precursor and surface growth species' mass fractions [37–40].

The reactor used in Rocha et al.'s 2019 experiments [9] was a porous media flat burner type, while in the Chemkin simulation, the available types were the batch, constant volume, constant pressure reactor, perfectly/partially stirred, and plugged flow reactors. In our predictions, we assumed an equilibrium (adiabatic) perfectly stirred reactor for simplicity. However, NH<sub>3</sub>NG predictions still largely agreed with the literature values. Another feature that differentiates our work from other literature mechanisms (i.e., those shown in Figures 7 and 8) is that the full mechanism (the Modified Konnov Mechanism, 132 species and 1238 reactions) used in this work was a combination of Konnov's mechanism and the USCII mechanism, while others are in the family of the Konnov mechanism for ammonia/methane combustion. NH<sub>3</sub>NG allowed the simulation of heavier hydrocarbons, such

as ethane and propane, and also had a better capability to predict soot emission with soot precursors  $C_2H_2$  and  $C_2H_4$  using the Moss–Brookes' equation in ANSYS Fluent [38,39].

In future work,  $NH_3NG$  can be used in ANSYS Fluent CFD simulations to further study the combustion process. For example, 3-D CFD simulations for various types of low  $NO_x$  and 2-stage burners that are suitable for modern gas/supercritical- $CO_2$  turbines and ICE applications can be performed [43,44].  $NO_x$ /soot/ $CO$ /unburnt fuel/VOC emissions under various equivalence ratios,  $NH_3$  to NG, NG composition, fuel flow rate, and air/fuel mixing patterns, can be estimated using ANSYS Fluent. CFD features, such as lean blow-off (LBO), can be used to investigate injection patterns and flame stability [46].

The developed  $NH_3NG$  Chemkin files are available from the corresponding author upon request.

## 5. Conclusions

A fuel mixture of ammonia and natural gas provides clean, low-carbon energy to run gas turbines and internal combustion engines for power generation, railroad/truck transportation, marine shipping, and commercial aviation. Reduced mechanisms are required in certain CFD software and can save computer time and storage in others for 3D CFD combustion applications. The newly proposed  $NH_3NG$  reduced mechanism can be employed in CFD works for the prediction of  $NO_x$ ,  $CO$ , and soot emissions involving ammonia and natural gas combustion. Soot emission can be predicted by applying the Moss–Brookes–Hall model using soot precursor species.

The prediction errors for  $NO_x$  and  $CO$  emissions associated with the use of the  $NH_3NG$  mechanism for ammonia–natural gas mixtures were also minimal (abs. error 5%) in comparison to the full Modified Konnov mechanism (a combination of the Konnov mechanism and the USCII mechanism). The  $NH_3NG$  reduced mechanism was validated with experimental laminar flame speed, ignition delay, adiabatic temperature, and  $NO_x$  and  $CO$  emissions' data.

The effect of ammonia in such fuel mixtures was also analyzed by comparing the Laminar flame speeds of the reduced mechanism to values found in the literature. An increase in the ammonia concentration in such a fuel mixture decreased the laminar flame speed of the combustion flame. An average absolute error of 7.7% was obtained for the laminar flame speed prediction, which is well within the reported experimental uncertainty of 10% [28]. The  $R^2$  between prediction and data was 0.985. The ignition delay time of the  $NH_3NG$  mechanism also agrees with the experimental data found in literature. An increase in the ammonia concentration in such a fuel mixture increased the ignition delay of the combustion flame. An average ignition delay prediction error of 13% was also within typical experimental data uncertainties (10–20%). The predictions of adiabatic temperatures were within 1 °C. Similar to all mechanisms in the literature, the present work overpredicted  $NO_x$  and  $CO$  emissions in relation to the published data [9,16,20,21]. Overall, the predictions from the  $NH_3NG$  mechanism are in line with other literature mechanisms. Compared to other mechanisms in the literature, the predicted  $CO$  emissions from  $NH_3NG$  were higher (further from the experimental data), while the predicted  $NO_x$  emissions were lower (closer to the experimental data).

**Author Contributions:** A.R.K. performed the literature review, validation of the reduced mechanism, and writing. V.D.D. contributed to the reduction of the full Modified Konnov Mechanism to  $NH_3NG$ . D.H.C. worked on the discussion, conclusion, and writing. All authors have read and agreed to the published version of the manuscript.

**Funding:** This work was supported by the Texas Air Research Center (TARC Grant #110LUB0179A). TARC was not involved in study design, in the collection, analysis, and interpretation of data, in the writing of the report, and in the decision to submit the article for publication.

**Institutional Review Board Statement:** Not applicable.

**Informed Consent Statement:** Not applicable.

**Data Availability Statement:** Not applicable.

**Conflicts of Interest:** The authors declare no conflict of interest.

### Glossary

ICE	Internal Combustion Engines
NG	Natural Gas
LNG	Liquified Natural Gas
VOC	Volatile Organic Compound
CFD	Computational Fluid Dynamics
RPA	Reaction Path Analyzer
PSR	Perfectly Stirred Reactor

### References

1. Trop, P.; Goricanec, D. Comparisons between energy carriers' productions for exploiting renewable energy sources. *Energy* **2016**, *108*, 155–161. [CrossRef]
2. Available online: [https://www.engineeringtoolbox.com/ammonia-pressure-temperature-d\\_361.html](https://www.engineeringtoolbox.com/ammonia-pressure-temperature-d_361.html) (accessed on 25 February 2023).
3. Sartbaeva, A.; Kuznetsov, V.L.; Wells, S.A.; Edwards, P.P. Hydrogen Nexus in a Sustainable Energy Future. *Energy Environ. Sci.* **2008**, *1*, 79–85. [CrossRef]
4. Natural Gas Specs Sheet. Available online: [https://www.naesb.org/pdf2/wgq\\_bps100605w2.pdf](https://www.naesb.org/pdf2/wgq_bps100605w2.pdf) (accessed on 25 February 2023).
5. Loz, B. *First Ammonia-Powered Jet Flight in 2023: A Roadmap to Clean Aviation*; New Atlas: Oklahoma City, OK, USA, 2022.
6. Sonal, P. Ammonia Gas Turbine Combustion Has Economic Potential, GE-IHI Study Suggests. Power. 2023. Available online: [https://www.powermag.com/ammonia-gas-turbine-combustion-has-economic-potential-ge-ihl-study-suggests/?oly\\_enc\\_id=1127F6602090B1F](https://www.powermag.com/ammonia-gas-turbine-combustion-has-economic-potential-ge-ihl-study-suggests/?oly_enc_id=1127F6602090B1F) (accessed on 23 February 2023).
7. Uchida, M.; Ito, S.; Suda, T.; Fujimori, T. Performance of Ammonia/Natural Gas Co-Fired Gas Turbine with 2-Stage Combustor, 367d. In Proceedings of the AIChE Annual Meeting, Orlando, FL, USA, 10–15 November 2019.
8. Rocha, R.; Costa, M.; Bai, X. Combustion and emission characteristics of ammonia under conditions relevant to modern gas turbines. *Combust. Sci. Technol.* **2021**, *193*, 2514–2533. [CrossRef]
9. Rocha, R.; Ramos, C.; Costa, M.; Bai, X. Combustion of  $\text{NH}_3/\text{CH}_4/\text{Air}$  and  $\text{NH}_3/\text{H}_2/\text{Air}$  Mixtures in a Porous Burner: Experiments and Kinetic Modeling. *Energy Fuels* **2019**, *33*, 12767–12780. [CrossRef]
10. Konnov, A.A. Implementation of the NCN pathway of prompt-NO formation in the detailed reaction mechanism. *Combust. Flame* **2009**, *156*, 2093–2105. [CrossRef]
11. Glarborg, P.; Miller, J.A.; Ruscic, B.; Klippenstein, S.J. Modeling nitrogen chemistry in combustion. *Prog. Energy Combust. Sci.* **2018**, *67*, 31–68. [CrossRef]
12. Mendiara, T.; Glarborg, P. Ammonia chemistry in oxy-fuel combustion of methane. *Combust. Flame* **2009**, *156*, 1937–1949. [CrossRef]
13. Han, X.; Lavadera, M.L.; Konnov, A.A. An experimental and kinetic modeling study on the laminar burning velocity of  $\text{NH}_3+\text{N}_2\text{O}+\text{air}$  flames. *Combust. Flame* **2021**, *228*, 13–28. [CrossRef]
14. Gianluca, C.; Vladimir, A.; Alekseev, A.; Konnov, A. An experimental and kinetic study of propanal oxidation. *Combust. Flame* **2018**, *197*, 11–21.
15. Wang, Z.; Han, X.; He, Y.; Zhu, R.; Zhu, Y.; Zhou, Z.; Cen, K. Experimental and kinetic study on the laminar burning velocities of  $\text{NH}_3$  mixing with  $\text{CH}_3\text{OH}$  and  $\text{C}_2\text{H}_5\text{OH}$  in premixed flames. *Combust. Flame* **2021**, *229*, 111392. [CrossRef]
16. The San Diego Mechanism: Chemical-Kinetic Mechanisms for Combustion Applications/Nitrogen Chemistry, Mechanical and Aerospace Engineering (Combustion Research), University of California, San Diego. Available online: <https://web.eng.ucsd.edu/mae/groups/combustion/mechanism.html> (accessed on 25 February 2023).
17. Wang, H.; You, X.; Joshi, A.V.; Davis, S.G.; Laskin, A.; Egolfopoulos, F.; Law, C.K. *USC Mech Version II. High-Temperature Combustion Reaction Model of  $\text{H}_2/\text{CO}/\text{C}_1\text{-C}_4$  Compounds*; CERFACS Chemistry: Toulouse, France, 2007.
18. CERFACS Chemistry 2023. USC II Detailed Mechanism. Available online: <https://chemistry.cerfacs.fr/en/chemical-database/mechanisms-list/usc-ii-mechanism/> (accessed on 25 February 2023).
19. Smith, G.P.; Tao, Y.; Wang, H. Foundational Fuel Chemistry Model Version 1.0 (FFCM-1). Available online: <https://web.stanford.edu/group/haiwanglab/FFCM1/pages/FFCM1.html> (accessed on 25 February 2023).
20. Tian, Z.; Li, Y.; Zhang, L.; Glarborg, P.; Qi, F. An experimental and kinetic modeling study of premixed  $\text{NH}_3/\text{CH}_4/\text{O}_2/\text{Ar}$  flames at low pressure. *Combust. Flame* **2009**, *156*, 1413–1426. [CrossRef]
21. Okafor, E.C.; Naito, Y.; Colson, S.; Ichikawa, A.; Kudo, T.; Hayakawa, A.; Kobayashi, H. Experimental and numerical study of the laminar burning velocity of  $\text{CH}_4\text{-NH}_3\text{-air}$  premixed flames. *Combust. Flame* **2018**, *187*, 185–198. [CrossRef]
22. Mathieu, O.; Petersen, E.L. Experimental and modeling study on the high-temperature oxidation of ammonia and related NOx chemistry. *Combust. Flame* **2015**, *162*, 554. [CrossRef]
23. Hayakawa, A.; Goto, T.; Mimoto, R.; Arakawa, Y.; Kudo, T.; Kobayashi, H. Laminar burning velocity and Markstein length of ammonia/air premixed flames at various pressures. *Fuel* **2015**, *159*, 98–106. [CrossRef]

24. Ramos, C.F.; Shu, B.; Fernandes, R.X.; Costa, M. Ignition Delay Times of Diluted Mixtures of Ammonia/Methane at Elevated Pressures. paper 367 c. In Proceedings of the Ammonia Energy Conference & AIChE Annual Meeting, Orlando, FL, USA, 12–14 November 2019.
25. Wang, S.; Wang, Z.; He, Y.; Sun, Z.; Liu, Y.; Zhu, Y.; Costa, M. *Laminar Burning Velocity and NO<sub>x</sub> Emission Measurements of NH<sub>3</sub>/CH<sub>4</sub>/Air and NH<sub>3</sub>/H<sub>2</sub>/Air Premixed Flames under Elevated Pressure*; The Combustion Institute: Pittsburgh, PA, USA, 2019.
26. Shu, B.; Ramos, C.F.; He, X.; Fernandes, R.X.; Costa, M. Experimental and modeling study on the auto-ignition properties of ammonia/methane mixtures at elevated pressures. *Proc. Combust. Inst.* **2021**, *38*, 261–268. [CrossRef]
27. Xiao, H.; Howard, M.S.; Valera-Medina, A.; Dooley, S.; Bowen, P. Reduced Chemical Mechanisms for Ammonia/Methane Co-Firing for Gas Turbine Applications. *Energy Procedia* **2017**, *105*, 1483–1488. [CrossRef]
28. Rocha, R.C.; Zhong, S.; Xu, L.; Bai, X.-S.; Costa, M.; Cai, X.; Kim, H.; Brackmann, C.; Li, Z.; Aldén, M. Structure and Laminar Flame Speed of an Ammonia/Methane/Air Premixed Flame under Varying Pressure and Equivalence Ratio. *Energy Fuels* **2021**, *35*, 7179–7192. [CrossRef] [PubMed]
29. Steffen, S.; Sabrina, S.; Lena, R.; Jacqueline, H.; Franziska, S.; Lubow, M.; Olaf, D.; Kohse-Höinghaus, K. Homogeneous conversion of NO<sub>x</sub> and NH<sub>3</sub> with CH<sub>4</sub>, CO, and C<sub>2</sub>H<sub>4</sub> at the diluted conditions of exhaust-gases of lean operated natural gas engines. *Int. J. Chem. Kinet.* **2021**, *53*, 213–229.
30. Huang, J.; Bushe, W.K. Experimental and Kinetic Study of Autoignition in Methane/Ethane/Air and Methane/Propane/Air Mixtures under Engine-Relevant Conditions. *Combust. Flame* **2006**, *144*, 74–88. [CrossRef]
31. Bowman, B.R.; Pratt, D.T.; Crowe, C.T. Effects of Turbulent Mixing and Chemical Kinetics on Nitric Oxide Production in a Jet-Stirred Reactor. *Symp. Int. Combust.* **1973**, *14*, 819–830. [CrossRef]
32. Kawka, L.; Juhász, G.; Papp, M.; Nagy, T.; Zsély, I.G.; Turányi, T. Comparison of detailed reaction mechanisms for homogeneous ammonia combustion. *J. Z. Phys. Chem.* **2020**, *234*, 1329–1357. [CrossRef]
33. Lou, H.; Martin, C.; Chen, D.; Li, X.; Li, K.; Vaid, H.; Tula, A.; Singh, K. Validation of a Reduced Combustion Mechanism for Light Hydrocarbons. *Clean Technol. Environ. Policy* **2012**, *14*, 737–748. [CrossRef]
34. Lou, H.; Chen, D.; Li, X.; Martin, C.; Richmond, P. *Flare Speciation and Air Quality Modeling*; TCEQ SEP Agreement No. 2009-009—Phase III, SEP Task 2-A Final Report; SEP: Austin, TX, USA, 2015.
35. Damodara, V.; Chen, D.; Lou, H.; Rasel, K.; Richmond, P.; Wang, A.; Li, X. Reduced Combustion Mechanism for C1-C4 Hydrocarbons and its Application in CFD Flare Modeling. *J. Air Waste Manag. Assoc.* **2017**, *67*, 599–612. [CrossRef] [PubMed]
36. Chemkin 2019 R2. Chemistry Simulation Software. Available online: <https://www.ansys.com/products/fluids/ansys-chemkin-pro> (accessed on 25 February 2023).
37. ANSYS. *ANSYS Fluent User's Guide Release 2021 R1*; Theory Guide Release 2021 R1; ANSYS® Academic Research, Release 2021 R1; ANSYS Inc.: Canonsburg, PA, USA, 2021.
38. Brookes, S.J.; Moss, J.B. Prediction of Soot and Thermal Radiation in Confined Turbulent Jet Diffusion Flames. *Combust. Flame* **1999**, *116*, 486–503. [CrossRef]
39. Fenimore, C.P.; Jones, G.W. Oxidation of soot by hydroxyl radicals. *J. Phys. Chem.* **1967**, *71*, 593–597. [CrossRef]
40. ANSYS. Soot Model Theory. Available online: <https://www.afs.enea.it/project/neptunius/docs/fluent/html/th/node229.htm> (accessed on 25 February 2023).
41. Rigopoulos, S. Modelling of Soot Aerosol Dynamics in Turbulent Flow. *Flow Turbul. Combust.* **2019**, *103*, 565–604. [CrossRef]
42. Reaction Design. *Reaction Workbench 15131*; Reaction Design: San Diego, CA, USA, 2013.
43. Goodwin, H.M.D.; Speth, R. Cantera: An Object-Oriented Software Toolkit for Chemical Kinetics, Thermodynamics, and Transport Processes. Version 2.2.1. 2016. Available online: <http://www.cantera.org> (accessed on 10 April 2023).
44. Quadrennial Technology Review 2015. *Supercritical Carbon Dioxide Brayton Cycle*; Technology Assessments, Chapter 4; US Department of Energy: Washington, DC, USA, 2015.
45. Fernandes, D.; Wang, S.; Xu, Q.; Buss, R.; Chen, D. Process and Carbon Footprint Analyses of the Allam Cycle Power Plant Integrated with an Air Separation Unit. *Clean Technol.* **2019**, *1*, 325–340. [CrossRef]
46. ANSYS. *ANSYS Energico User's Guide 2020 R1*; ANSYS Inc.: Canonsburg, PA, USA, 2020.

**Disclaimer/Publisher's Note:** The statements, opinions and data contained in all publications are solely those of the individual author(s) and contributor(s) and not of MDPI and/or the editor(s). MDPI and/or the editor(s) disclaim responsibility for any injury to people or property resulting from any ideas, methods, instructions or products referred to in the content.